April 24, 2024

Abstract

two-dimensional problems into one-dimensional boundary problems, achieving dimensionality

Strong Generalizability: Based on our meticulously designed network architecture and

for operator learning. Lower dimension leads to fewer sampling points which will reduce the

tain other methods, such as those reliant on high-performance computing using GPUs, thereby

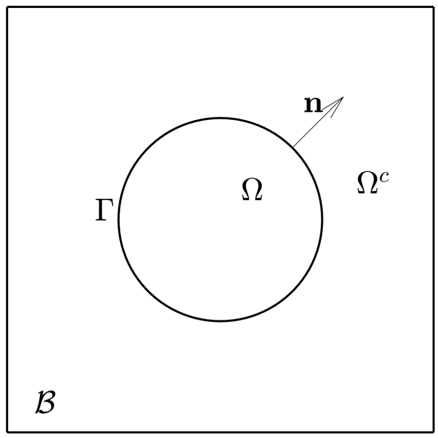

(3)

(4)

$$\int \frac{\partial G(\mathbf{y},\mathbf{x})}{\partial \mathbf{n_y}} \tag{5}$$

$$\int \tag{6}$$

$$\tag{7}$$

$$u(\mathbf{x}) = (W\varphi)(\mathbf{x}) + (Yf)(\mathbf{x}), \quad \mathbf{x} \in \Omega, \tag{8}$$

$$\widetilde{W}(\varphi)(\mathbf{x}) := (\frac{1}{2}\mathcal{I} + W)(\varphi)(\mathbf{x}), \quad \mathbf{x} \in \Gamma, \tag{9}$$

$$u \quad \widetilde{} \tag{10}$$

where $\{\mathbf{x}_i\}_{i=1}^{M}$ are discrete points on boundary Γ and $\widetilde{g_D}(\mathbf{x}) := g_D(\mathbf{x}) - (Yf)(\mathbf{x})$ need only

$\widetilde{}$

piecewise smooth function with discontinuities only existing at the interface Γ. We denote

$$\tag{12}$$

$$\tag{13}$$

work's input as $(\mathbf{x_1}, \mathbf{x_2}, ..., \mathbf{x_M})^T$ and $(\widetilde{g_D}(\mathbf{x_1}), \widetilde{g_D}(\mathbf{x_2}), ..., \widetilde{g_D}(\mathbf{x_M}))^T$, where $\mathbf{x_i} = (x_{i,1}, x_{i,2})^T$ is

of networks $\mathcal{N}_\Omega$ as $(k_1, k_2, ..., k_n)^T$ and $(\widetilde{g_D}(\mathbf{x_1}), \widetilde{g_D}(\mathbf{x_2}), ..., \widetilde{g_D}(\mathbf{x_M}))^T$.

which receives $(\widetilde{g_D}(\mathbf{x_1}), ..., \widetilde{g_D}(\mathbf{x_M}))^T$ as input and outputs $(\varphi(\mathbf{x_1}), ..., \varphi(\mathbf{x_M}))^T$, is outlined in appropriately chosen d.

$(\mathbf{x_1}, \mathbf{x_2}, ..., \mathbf{x_M})^T$, boundary parameters such as r_a, r_b, or operator parameters like $k_1, k_2, ..., k_n$.

specific network.

ONet [38].

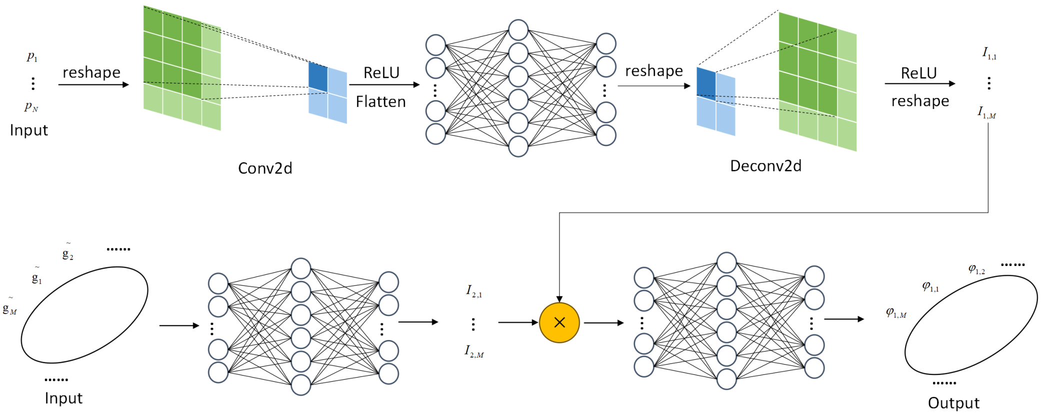

$$\sum^{n} ||\mathcal{N}_{\mathcal{L},\Omega}(\widetilde{g_D}_i;\Theta_{\mathcal{L},\Omega}) - \varphi_i||_2^2, \tag{14}$$

where $\widetilde{g_D}_i = (\widetilde{g_D}_i(\mathbf{x_1}), \widetilde{g_D}_i(\mathbf{x_2}), ..., \widetilde{g_D}_i(\mathbf{x_M}))^T$, $\varphi_i = (\varphi_i(\mathbf{x_1}), \varphi_i(\mathbf{x_2}), ..., \varphi_i(\mathbf{x_M}))^T$ are the i-th

$$(15)$$

$$\left\{ \begin{array}{l}))](x^2+y^2)^5 \\ ))(x^2+y^2)^5 \end{array} \right. \tag{16}$$

	$\begin{bmatrix} \\ 1.1E-2 \\ 1.3E-2 \end{bmatrix}$	$\begin{bmatrix} 1.1E-4 \\ 1.2E-4 \\ \ \end{bmatrix}$	$\begin{bmatrix} 2.1E-4 \\ 2.3E-4 \\ \ \end{bmatrix}$	$\begin{bmatrix} 1.9E-4 \\ 1.7E-4 \\ \ \end{bmatrix}$
	$\begin{bmatrix} 2.5E-4 \\ 5.2E-4 \\ \ \end{bmatrix}$	$\begin{bmatrix} 6.3E-5 \\ 9.4E-5 \\ 6.0E-4 \end{bmatrix}$	$\begin{bmatrix} 1.3E-5 \\ \ \\ 1.7E-4 \end{bmatrix}$	$\begin{bmatrix} 3.1E-6 \\ 6.2E-6 \\ 4.5E-5 \end{bmatrix}$
	$\begin{bmatrix} 2.5E-4 \\ 5.2E-4 \\ \ \end{bmatrix}$	$\begin{bmatrix} 6.3E-5 \\ 9.4E-5 \\ 6.9E-5 \end{bmatrix}$	$\begin{bmatrix} 1.3E-5 \\ \ \\ 1.7E-4 \end{bmatrix}$	$\begin{bmatrix} 3.1E-6 \\ 6.2E-6 \\ 4.5E-5 \end{bmatrix}$

$_{\text{act}}, p_{\text{exact}})$.

grids of size 128×128, 256×256, 512×512 and 1024×1024 using Strategy 1 is merely 0.1280s,

S_m, S_c.

(S_m, S_c)	$(3, 0.20)$	$(4, 0.10)$	$(5, 0.05)$	$(6, 0.15)$

$$\left\{ \quad \right. \tag{17}$$

(r_a, r_b)	$(0.8, 0.8)$	$(1.0, 1.1)$	$(1.1, 1.0)$	$(1.1, 1.1)$
	$\begin{bmatrix} 7.6E-4 \\ 3.5E-4 \\ \end{bmatrix}$	$\begin{bmatrix} 5.4E-4 \\ 7.7E-4 \\ \end{bmatrix}$	$\begin{bmatrix} 5.0E-4 \\ 4.8E-4 \\ \end{bmatrix}$	$\begin{bmatrix} 7.6E-4 \\ 7.2E-4 \\ \end{bmatrix}$
	$\begin{bmatrix} 5.2E-5 \\ 3.5E-5 \\ \end{bmatrix}$	$\begin{bmatrix} 3.5E-5 \\ \\ 6.9E-4 \end{bmatrix}$	$\begin{bmatrix} \\ \\ 5.5E-4 \end{bmatrix}$	$\begin{bmatrix} \\ 3.2E-5 \\ 5.5E-4 \end{bmatrix}$
	$\begin{bmatrix} 5.2E-5 \\ 3.5E-5 \\ \end{bmatrix}$	$\begin{bmatrix} 3.5E-5 \\ \\ 6.9E-4 \end{bmatrix}$	$\begin{bmatrix} \\ \\ 5.5E-4 \end{bmatrix}$	$\begin{bmatrix} \\ 3.2E-5 \\ 5.5E-4 \end{bmatrix}$

$_{\text{act}}, p_{\text{exact}})$.

designated a dumbbell-shaped area, as depicted in figure 3. Specifically, $\partial\Omega$ is a periodic C^2

with varying values of κ. For illustration, numerical solutions obtained through Strategy 1 and Strategy 2, using a grid size of 256×256 and a coefficient $\kappa = 3$, are depicted in figure 3.

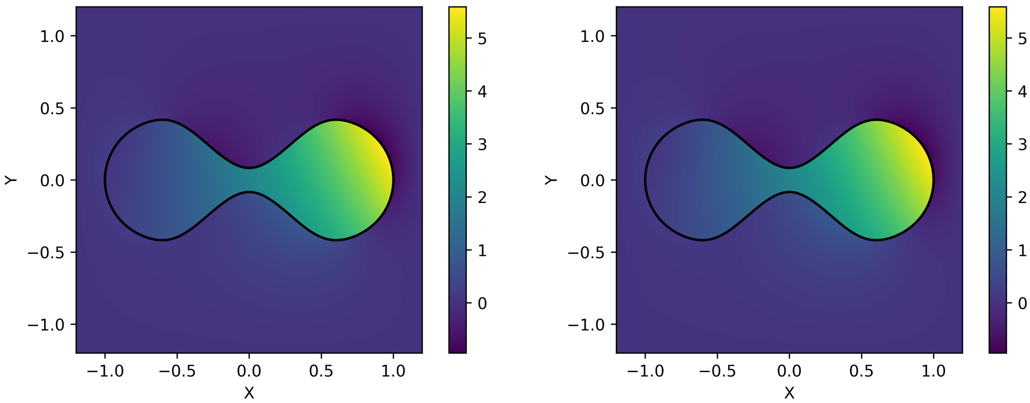

computational domain. Specifically, beyond varying the parameter κ within the range $[0.5, 3.0]$, the computational domain Ω can also undergo transformations involving rotation by an angle

Ω_0 is similarly obtained through cubic spline interpolation of a set of control points (which is recorded in Appendix C.1 for details), and $\alpha \in [0, 2\pi]$, $r \in [0.6, 1]$. In this case, both κ and

values α, r and κ. For illustration, numerical solutions obtained through Strategy 1 and Strategy

, $r = 0.7$ and $\kappa = 2.8$, are depicted in figure 4.

	$, 0.7, 2.8)$	$(\frac{\pi}{4}, 0.7, 2.8)$	$(\frac{\pi}{6}, 0.71, 0.9)$	$($

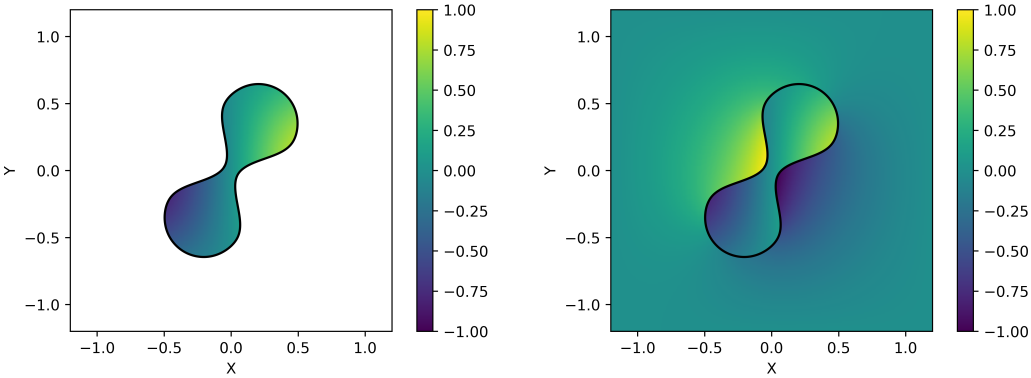

Figure 4: Exact solution and Numerical solution of Modified Helmholtz equation 2 given by original PDE.

exhibits remarkable accuracy, while its computational speed is astonishing, consuming less than

(18)

here $\mathbf{u} = \left(u^{(1)}, u^{(2)}\right)^T$, $\mathbf{f} = \left(f^{(1)}, f^{(2)}\right)^T$ represent displacement variable and external force,

(19)

coefficients λ and μ is given by Young's modulus E and Poisson's ratio ν:

$$(20)$$

$+xy$ and $u^{(2)} = \cos x \sin y + xy$, applied to the heart-shaped domain with various (E, ν) parameter values. As an example, the numerical solution obtained through Strategy 2, employing a grid size of 256×256 and coefficients $(E, \nu) = (5.5 \times 10^8, 0.4)$, is depicted in figure 5.

(E, ν)	(3E08, 0.4)	(5.2E08, 0.35)	(5.5E08, 0.4)	(9E08, 0.36)
	$\begin{bmatrix} 9.5E-4 \\ 8.5E-4 \end{bmatrix}$	$\begin{bmatrix} 5.1E-4 \\ 4.9E-4 \end{bmatrix}$	$\begin{bmatrix} 9.6E-4 \\ 8.5E-4 \end{bmatrix}$	
	$\begin{bmatrix} 1.4E-4 \\ 1.2E-4 \end{bmatrix}$	$\begin{bmatrix} 1.0E-4 \\ 8.9E-5 \end{bmatrix}$	$\begin{bmatrix} 1.4E-4 \\ 1.2E-4 \end{bmatrix}$	$\begin{bmatrix} 1.1E-4 \\ 9.3E-5 \end{bmatrix}$
	$\begin{bmatrix} 1.4E-4 \\ 1.2E-4 \end{bmatrix}$	$\begin{bmatrix} 1.0E-4 \\ 8.9E-5 \end{bmatrix}$	$\begin{bmatrix} 1.4E-4 \\ 1.2E-4 \end{bmatrix}$	$\begin{bmatrix} 1.1E-4 \\ 9.3E-5 \end{bmatrix}$

$(u$ $\quad$ $_{\text{act}})$.

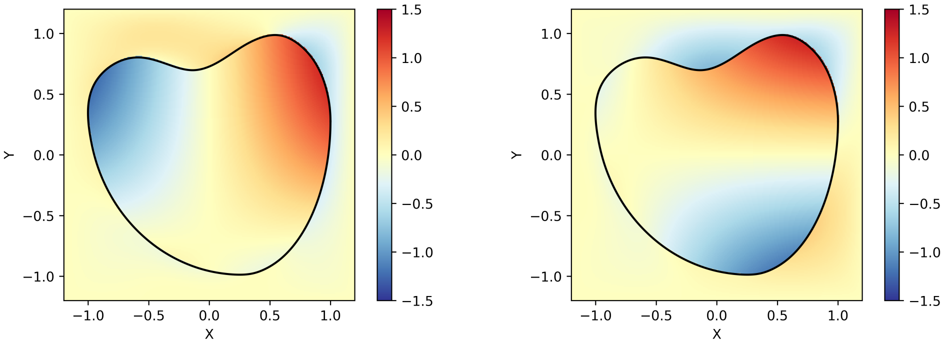

Displacement $u^{(1)}$.

Displacement $u^{(2)}$.

Figure 5: Numerical solution of the 2D Naiver equation 1 given by Strategy 2 in grid 256×256.

boundary with various $(\epsilon_1, \epsilon_{14}, \epsilon_{27})$ parameter values. As an example, the numerical solution

$(+0.05, +0.05, -0.1)$, is depicted in figure 6.

In this section, we allow for perturbations to be applied to certain control points that deter-

pabilities. Particularly noteworthy, both the error metrics and figure 6 representations illustrate

$(\epsilon_1, \epsilon_{14}, \epsilon_{27})$	(+0.05, +0.05, -0.1)	(-0.04, +0.02, 0)	(+0.02, -0.01, +0.06)

Table 10: Result of Naiver equation 2: comparison of accuracy and efficiency in solving Naiver

act).

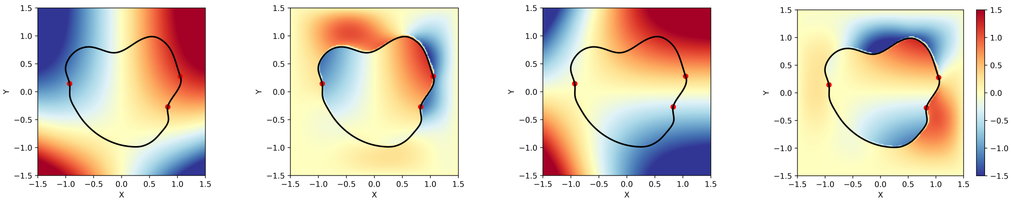

Acknowledgments

References

REFERENCES

[40] Nicholas H. Nelsen and Andrew M. Stuart. The random feature model for input-output

REFERENCES

REFERENCES

$$\mathcal{L}v(\mathbf{x}) = \mathcal{F}(\mathbf{x}), \quad \mathbf{x} \text{ in } \Omega \cup \Omega^c,$$

$$\int G(\mathbf{y},\mathbf{x})\psi(\mathbf{y})ds_{\mathbf{y}} \quad \text{for} \quad \mathbf{x} \in \Omega \cup \Omega^c.$$

$$\frac{\;}{2}\psi(\mathbf{x}) - \partial_{\mathbf{n}}(S\psi)(\mathbf{x}) + \partial_{\mathbf{n}}(Yf)(\mathbf{x}) = g_N(\mathbf{x}).$$

$$u(\mathbf{x}) = (Yf)(\mathbf{x}) - (S\psi)(\mathbf{x}), \quad x \in \Omega.$$

$$\partial_{\mathbf{n}} u \qquad \psi(\mathbf{x}_m) - \partial_{\mathbf{n}}(S\psi)(\mathbf{x}_m), \quad m = 1, 2, \cdots, M, \tag{26}$$

where $\{\mathbf{x}_i\}_{i=1}^{M}$ are control points on boundary Γ and $\hat{g}_N(\mathbf{x}_m) := g_N(\mathbf{x}_m) - \partial_{\mathbf{n}}(Yf)(\mathbf{x}_m)$, for $\mathbf{x}_m \in$

$$\partial_{\mathbf{n}} w^+(\mathbf{x}) = \lim_{z \to x, z \in \Omega} \partial_{\mathbf{n}} w(\mathbf{z}),$$

{0.000e+00, 8.333e-02}, {-1.944e-01, 1.698e-01}, {-3.889e-01, 3.302e-01},
{-5.833e-01, 4.167e-01}, {-7.917e-01, 3.608e-01}, {-9.442e-01, 2.083e-01},
{-1.000e+00, 0.000e+00}, {-9.442e-01, - 2.083e-01}, {-7.917e-01, - 3.608e-01},
{-5.833e-01, - 4.167e-01}, {-3.889e-01, - 3.302e-01}, {-1.944e-01, - 1.698e-01},
{0.000e+00, - 8.333e-02}, {1.944e-01, - 1.698e-01}, {3.889e-01, - 3.302e-01},
{5.833e-01, - 4.167e-01}, {7.917e-01, - 3.608e-01}, {9.442e-01, - 2.083e-01},
{1.000e+00, 0.000e+00}, {9.442e-01, 2.083e-01}, {7.917e-01, 3.608e-01},
{5.833e-01, 4.167e-01}, {3.889e-01, 3.302e-01}, {1.944e-01, 1.698e-01}.

{1.000e+00, 2.763e-01}, {9.639e-01, 5.482e-01}, {8.613e-01, 7.787e-01},
{7.076e-01, 9.328e-01}, {5.263e-01, 9.868e-01}, {3.070e-01, 9.118e-01},
{8.772e-02, 7.724e-01}, {-1.316e-01, 6.974e-01}, {-3.553e-01, 7.500e-01},
{-5.789e-01, 8.026e-01}, {-7.895e-01, 7.462e-01}, {-9.436e-01, 5.921e-01},
{-1.000e+00, 3.816e-01}, {-9.808e-01, 1.440e-01}, {-9.238e-01, - 8.645e-02},

{-8.308e-01, - 3.026e-01}, {-7.045e-01, - 4.980e-01}, {-5.488e-01, - 6.667e-01}, {-3.684e-01, - 8.035e-01}, {-1.689e-01, - 9.043e-01}, {4.381e-02, - 9.661e-01}, {2.632e-01, - 9.868e-01}, {4.271e-01, - 9.552e-01}, {5.829e-01, - 8.618e-01}, {7.226e-01, - 7.113e-01}, {8.392e-01, - 5.113e-01}, {9.270e-01, - 2.717e-01}, {9.815e-01, - 4.763e-03}.